**International Institute for
Applied Systems Analysis
www.iiasa.ac.at**

Robust Stabilization of Atmospheric Carbon within a Family of Uncertain Carbon Cycle Dynamics

Melnikov, N.

**IIASA Interim Report
September 2004**

Interim Report IR-04-053

Robust Stabilization of Atmospheric Carbon within a Family of Uncertain Carbon Cycle Dynamics

Nikolai Melnikov (melnikov@cs.msu.ru)

Approved by

Arkady Kryazhimskiy (kryazhim@iiasa.ac.at & kryazhim@mtu-net.ru)
Program Leader, Dynamic Systems

September 2004

Contents

Abstract

A recently developed robust stabilization method for uncertain dynamical systems is applied to the problem of stabilizing the atmospheric carbon concentration. The underlying uncertain carbon cycle dynamics is treated as a class of deterministic nonlinear dynamical systems, containing the "real" one, which is unknown. The stabilization methodology incorporates a special learning mechanism allowing to reduce the uncertainty. Relations between the learning rate and parameters of the emission control strategy are analyzed. The analysis is based on numerical simulations using, among others, basic IPCC emission scenarios.

About the Author

Nikolai Melnikov
Chair of Optimal Control
Faculty of Computational Mathematics & Cybernetics
Moscow State University, Vorobyevy Gory
Moscow 119899, Russia

Acknowledgments

Robust Stabilization of Atmospheric Carbon within a Family of Uncertain Carbon Cycle Dynamics

Nikolai Melnikov (melnikov@cs.msu.ru)

Introduction

The problem of the stabilization of the atmospheric carbon concentration is widely discussed in the context of global warming nowadays (see, e.g., Wigley, 2004). One of the key difficulties in solving this problem is the uncertainty of the physical model of the circulation of carbon in the biosphere. Since the carbon cycle process as well as its impacts on climate change are not well understood so far, it is reasonable to consider a "pool of admissible models" which contains the real one. A feedback stabilization procedure should be then model-robust, e.g., it should work for any admissible model, making use of an on-line information on the process. We briefly present this approach in Section 1.

In order to implement the approach, we apply the robust stabilization method suggested in Kryazhimskiy and Maksimov, 2003, 2004. The method is based on a special learning effect that allows to reduce the uncertainty gradually. A brief outline of the method is given in Section 2.

The aim of this paper is to analyze the relations of the learning rate to the cost for the updates of the basic emission scenario, the delay in the implementation of the scenario updates, and the target level of the atmospheric carbon concentration. In Section 3, we analyze these relations numerically for two sets of basic emission scenarios. One set of scenarios is designed through the use of a simple analytic expression determined by the total value of accumulated emission. The other set comprises emission scenarios suggested by the Intergovernmental Panel on Climate Change (IPCC). Some open questions are discussed in Section 4.

1   Model

Carbon cycle models describe the process of the circulation of carbon across several reservoirs. In the "two well-mixed box" model (see Nordhaus, 1980; Svirezhev, *et al.*, 1999) the carbon-containing reservoirs are divided into two groups according to the speed of their reaction to the carbon emission; those that respond quickly to the carbon emission (the atmosphere, biosphere, mixed layer of ocean, etc.) and those where the deposition is slow (the deep ocean). The model dynamics is represented by the following system of nonlinear differential equations:

$$\begin{aligned}
\dot{x} &= \varphi(t) + g(x, y), \\
\dot{y} &= -g(x, y)
\end{aligned} \tag{1}$$

where x and y stand for the deviations of the total mass of carbon from its pre-industrial level. The following table provides a more precise description of the variables:

$x(t)$ –   elevation of the average CO_2 concentration in the atmosphere
and quick response reservoirs (the deviation from the pre-industrial level);

$y(t)$ –   elevation of the average CO_2 concentration in deep ocean
(the deviation from the pre-industrial level);

$\varphi(t)$ –   anthropogenic CO_2 emission into the atmosphere per year.

A common assumption is that the anthropogenic emission $\varphi(t)$ tends to zero as time grows to infinity; this is a transformation of the view that in the future new energy carriers will be utilized. Once the emission is fixed, two types of uncertainty are present in the model: the dynamics $g(x, y)$ and the initial states

$$x(0) = x^0 \qquad y(0) = y^0. \tag{2}$$

Each admissible model (1), (2) is determined by an (unknown) function $g(x, y)$ decreasing in x and increasing in y, and initial values x^0, y^0 measured with some errors. The stabilization problem, in which $\varphi(t)$ acts as a control, consists in reaching a prescribed target value for the atmospheric carbon concentration:

$$\lim_{t \to \infty} x(t) = \hat{x}. \tag{3}$$

A control strategy is constructed using the observations of the actual atmospheric carbon concentration $x(t)$ evolving in time.

Prior to discussing the proposed method for stabilizing an uncertain dynamical system, let us make a small remark on the stabilization of a system without uncertainty. The solution to equation (1) satisfies the balance equation

$$x(t) + y(t) = x^0 + y^0 + \Phi(t), \qquad \Phi(t) = \int_0^t \varphi(\tau) \, d\tau, \tag{4}$$

where $\Phi(t)$ is the accumulated emission. Eliminating $y(t)$ from (1), one comes to

$$\dot{x} = \varphi(t) + g(x, -x + x^0 + y^0 + \Phi(t)). \tag{5}$$

Provided the accumulated emission tends to a saturation level $\bar{\Phi}$ as time goes to infinity, the latter equation determines the "limit dynamics":

$$\dot{x} = g(x, -x + x^0 + y^0 + \bar{\Phi}). \tag{6}$$

If the "limit dynamics" has the unique rest point, then given a target value $\hat{x}$, one can identify the corresponding saturation level for the accumulated emission $\hat{\Phi}$ from the equation

$$g(\hat{x}, -\hat{x} + x^0 + y^0 + \hat{\Phi}) = 0. \tag{7}$$

Any emission scenario with this saturation level stabilize $x(t)$ at the target level $\hat{x}$ as time approaches infinity.

The uncertainty in the system dynamics g and in the initial values x^0 and y^0 does not allow us to use this simple method for finding a desired emission scenario. The task appears to be more challenging.

2   Method

Here we introduce the notation and briefly outline the method for stabilizing an uncertain system of form (1). A proof of the convergence of the method as well as a more general setting can be found in Kryazhimskiy and Maksimov, 2003, 2004.

¿From now on, $\varphi(t)$ stands for the basic emission scenario and $u(t)$ stands for the scenario correction input. In this view, system (5) is modified into

$$\begin{aligned}
\dot{x} &= \varphi(t) + u(t) + g(x, y), \\
\dot{y} &= -g(x, y).
\end{aligned} \tag{8}$$

The class of admissible models is defined as follows. Each admissible function $g(x, y)$ is continuously differentiable; moreover, it vanishes at the origin, $g(0, 0) = 0$, monotonically decreases in x, monotonically increases in y and satisfies the growth constraints

$$-a_2 \leq \frac{\partial g}{\partial x} \leq -a_1, \quad b_1 \leq \frac{\partial g}{\partial y} \leq b_2$$

with some fixed positive constants a_1, a_2, b_1, b_2. Each admissible initial state satisfied interval constraints:

$$x^- \leq x^0 \leq x^+, \qquad y^- \leq y^0 \leq y^+.$$

Introducing the new control variable

$$w(t) = \int_0^t u(\tau)\, d\tau,$$

analogously to (5) we get

$$\dot{x}(t) = f(t, x(t), y(t), w(t), \dot{w}(t)),$$

where

$$f(t, x, w, \dot{w}) = \varphi(t) + \dot{w} + g(x, -x + x^0 + y^0 + w + \Phi(t)).$$

We also assume that

$$\lim_{t \to \infty} \dot{w}(t) = 0, \qquad \lim_{t \to \infty} w(t) = \bar{w}.$$

The contoller's task is to form an admissible control $w(t)$ such that the rest point $\bar{x}$ for the "limit dynamics"

$$\dot{x}(t) = \bar{f}(x(t), w(t)),$$

where

$$\bar{f}(x, w) = g(x, -x + x^0 + y^0 + \bar{w} + \bar{\Phi}),$$

takes the prescribed value $\hat{x}$. The control strategy is implemented as a sequence of extensions of current controls; each new control $w_{m+1}(t)$ extends the previous control $w_m(t)$ beyond some t_m, i.e., coincides with $w(t)$ on the interval $[0, t_m)$.

At the initial time $t = 0$ the controller selects an initial admissible control $w_0(t)$ and estimates the inconsistency subset $\bar{W}_0$ that comprises all limit values $\bar{w}$ that are unable to solve the stabilization problem. The motion of the real system starts under $w_0(t)$ and goes along a trajectory $x_0(t)$. At each time $t \geq 0$ the controller observes $x_0(t)$ and decides whether $w_0(t)$ must be switched to another extension $w_1(t)$. If the controller decides to switch at a t_1^*, he/she updates the initial inconsistency set $\bar{W}_0$, forming a $\bar{W}_1$, fixes a delay $\delta(t_1^*) \geq 0$ and switches the admissible control from $w_0(t)$ to $w_1(t)$ at time $t_1 = t_1^* + \delta(t_1^*)$.

The performance of m steps of the control process results in the formation of admissible controls $w_0(t), w_1(t), \ldots, w_m(t)$ switched on sequentially at $0, t_1, \ldots, t_m$ and a set estimate $\bar{W}_m$ of inconsistent limit values of admissible controls. On $[t_i, t_{i+1})$ the real system goes along a trajectory $x_i(t)$ corresponding to $w_i(t)$ ($i = 0, 1, \ldots, m - 1$). At each time $t \geq t_m$ the controller observes $x_m(t)$ and decides whether $w_m(t)$ must be switched to another extension. If the controller decides to switch at a time t_{m+1}^*, he/she formes $\bar{W}_{m+1}$ instead of $\bar{W}_m$, fixes a delay $\delta(t_{m+1}^*) \geq 0$ and switches from $w_m(t)$ to $w_{m+1}(t)$ at time $t_{m+1} = t_{m+1}^* + \delta(t_{m+1}^*)$. The time t_{m+1}^*, at which

the controller decides to switch, will further be called the time of the receipt of the *inconsistency signal*. Note that the receipt of the inconsistency signal at time t_{m+1}^* implies that the limit value $\bar{w}_m$ is inconsistent with the target value $\hat{x}$. Therefore, at time t_{m+1}^* the controller can update $\bar{W}_m$, i.e., form $\bar{W}_{m+1}$, by adding $\bar{w}_m$ (and possibly some other elements).

The sequence $(t_m, w_m(t))$ (generally infinite) of switching times and corresponding extensions forms a control flow; and the sequence $(t_m, x_m(t))$ forms a trajectory flow. The entire trajectory $x(t)$ is formed through pasting together the "flow" trajectories at the switching times: $x(t) = x_m(t)$ for all $t_m \le t \le t_{m+1}$ (or $t_m \le t < \infty$ if t_m is the latest switching time). Within this pattern, major technical tasks are obviously to identify the inconsistency of each current control $w_m(t)$ and to choose its extension $w_{m+1}(t)$ upon the receipt of the inconsistency signal.

An important fact used for the identification of an inconsistency signal is the existence of a positive continuous *calibration function* $\nu(t)$ that vanishes at infinity and satisfies

$$|x_m(t) - \bar{x}_m| \le \nu(t - t_m), \qquad t_m \le t \tag{9}$$

for the trajectory flow $(t_m, x_m(t))$ corresponding to any admissible model (see Kryazhimskiy and Maksimov, 2003, 2004). Once the target value $\hat{x}$ is given, the calibration function $\nu(t)$ defines a *funnel* around $\hat{x}$, located between $\hat{x} - \nu(t)$ and $\hat{x} + \nu(t)$. Then either the trajectory $x_m(t)$ never leaves the funnel, and thus goes to the target value automatically, or it crosses one of the ridges. In the latter case, the first instant t_{m+1}^* of crossing is identified as the time of the receipt of the inconsistency signal.

Admissible control flows $(t_m, w_m(t))$ are defined so that the limit values of the extensions $w_m(t)$ are uniformly bounded:

$$w^- \le \bar{w}_m \le w^+,$$

and the bounds w^- and w^+ are calculated in advance using the constraints on the class of admissible models. Namely, the interval (w^-, w^+) is chosen so that it contains zero and the inequalities

$$g(\hat{x}, -\hat{x} + x^0 + y^0 + \bar{\Phi}) + b_1 w^- \le 0, \tag{10}$$

$$g(\hat{x}, -\hat{x} + x^0 + y^0 + \bar{\Phi}) + b_1 w^+ \ge 0 \tag{11}$$

hold for all admissible models. Moreover, as each admissible control $w(t)$ vanishes at infinity, it is assumed that each extension $w_m(t)$ is constrained by $|\dot{w}_m(t)| \le \gamma(t_m)$, where $\lim_{t\to\infty} \gamma(t) = 0$. This inequality is ensured if we set $\dot{w}_m(t) = \pm\gamma(t_m)$ for $t_m \le t \le \tau_m$ and $\dot{w}_m(t) = 0$ otherwise. Thus we fix the structure of the extensions $w_m(t)$ so that the absolute value $|\dot{w}_m(t)|$ takes its maximal value till the stopping time τ_m and vanishes afterwards. It is also assumed that each extension starts not earlier than the previous one is terminated: $t_{m+1} = t_{m+1}^* + \delta(t_{m+1}^*) \ge \tau_m$.

Let us specify the algorithm. It starts with $\bar{W}_0 = \emptyset$, $w_0^- = w^-$ and $w_0^+ = w^-$ and in each period m produces an inconsistency set W_m that complements some interval $[w_m^-, w_m^+]$ to $[w^-, w^+]$. The interval $[w_m^-, w_m^+]$ represents the current *uncertainty interval*, containing all adimissible limit values of the controls, which are (so far) consistent with the tarject value $\hat{x}$. In each period m the inconsistency set W_m is transformed into a larger set W_{m+1}. Accordingly, the current uncertainty interval $[w_m^-, w_m^+] = [w^-, w^+] \setminus \bar{W}_m$ is transformed into a smaller one, $[w_{m+1}^-, w_{m+1}^+] = [w^-, w^+] \setminus \bar{W}_{m+1}$. This transformation, which reduces the uncertainty, acts as a step in a *learning procedure* that accompanies the stabilization process. In the transformation of W_m into W_{m+1} at time t_{m+1}^* (at which $x_m(t)$ crosses one of the ridges of the funnel (9)) the fact, which of the ridges is crossed, is crucial:

$$x_m(t_{m+1}^*) = \hat{x} - \nu(t_{m+1}^* - t_m) \qquad \text{(the funnel's lower ridge is crossed)},$$

or

$$x_m(t_{m+1}^*) = \hat{x} + \nu(t_{m+1}^* - t_m) \qquad \text{(the funnel's upper ridge is crossed)}$$

4

Let us consider the case where the trajectory $x_m(t)$ crosses the lower ridge of the funnel. In this case $\bar{x} > \hat{x}$; since the limit value $\bar{x}$ increases in $\bar{w}$, the whole interval $[w_m^+, \bar{w}_m]$ is inconsistent with the target value $\hat{x}$; therefore we implement the largest possible emission reduction rate, $\dot{w}_{m+1}(t) = -\gamma(t_{m+1})$, and set $\bar{W}_{m+1} = \bar{W}_m \cup [w_m^+, \bar{w}_m]$. The limit level for the extension $w_{m+1}(t)$ is assigned as the median of the compliment to the inconsistency set: $\bar{w}_{m+1}(t) = (\bar{w}_m + w_m^-)/2$. Similarly, for the case where the upper ridge of the funnel is crossed, we allow the maximal possible emission growth rate, $\dot{w}_{m+1}(t) = \gamma(t_{m+1})$, and set $\bar{W}_{m+1} = \bar{W}_m \cup [\bar{w}_m, w_m^+]$ and $\bar{w}_{m+1}(t) = (w_m^+ + \bar{w}_m)/2$.

Note that in both cases, the uncertainty is reduced two times; more specifically, the uncertainty interval $[w_m^-, w_m^+]$ is reduced to the new one, $[w_{m+1}^-, w_{m+1}^+]$, whose length is two times shorter.

A theoretical result states that $\bar{w}_m \to \hat{w}$ and $\bar{x}_m \to \hat{x}$.

3 Results

3.1 Linear models

In our numerical simulations we use uncertain linear models of the form (see Nordhaus, 1980)

$$\begin{aligned} \dot{x} &= \varphi(t) - \alpha x + \beta y, \\ \dot{y} &= \alpha x - \beta y, \end{aligned} \tag{12}$$

where positive α and β are uncertain transfer coefficients. The values of α and β as well as the initial states x^0 and y^0 range, respectively, in intervals $[a_1, a_1]$, $[b_1, b_2]$, $[x^-, x^+]$ and $[y^-, y^+]$, which account for the uncertainty. The graph of the limit atmospheric carbon concentration $\hat{x}$ as a function of the transfer coefficients, for the initial states $x^0 = 145\ GtC$, $y^0 = 76\ GtC$ (Svirezhev et al., 1999) is presented in Figure 1. We see that the limit atmospheric carbon concentration $\hat{x}$ decreases in α and increases in β, and if the basic emission scenario is not corrected, the spread of admissible limit values is considerable.

3.2 Exponential emission scenarios

In the first series of runs (see Figure 2), we take an exponentially decreasing basic emission scenario: $\varphi(t) = \bar{\Phi} \exp(-t)$. For the total accumulated emission we take $\bar{\Phi} = 500\ GtC$ (see Svirezhev et al., 1999). We also assume that $w_0 \equiv 0$, i.e., the basic scenario is not corrected before the first switching time. The upper bound for the correction inputs is set to be $\gamma(t) = 300/(1+t)$, and the delay δ is assigned as $10k$, where k is the current number of switches. The calibration function $\nu(t)$ can be found explicitly, however, to shorten the running time of the algorithm we take the crude estimate $\nu(t) = G \exp(-(\alpha + \beta)t)$ instead. The value of the parameter G depends on $\varphi(t)$; here we set $G = 600\ GtC$. The values of other parameters are given in Table 1. The intervals for the uncertain coefficients α and β and initial states x^0, y^0 are taken so that they contain the values given in Svirezhev et al., 1999 (Table 1, (a)); the latter values are assumed here to be the exact ones.

Figure 2 shows that the stabilization process depends considerably on the target value $\hat{x}$. It suggests that the greater is the difference between the target value $\hat{x}$ and the model's limit value $\bar{x}$, the higher is the oscillation amplitude of the atmospheric carbon concentration $x(t)$ as it goes to the target value.

3.3 IPCC scenarios

In order to make the simulations more realistic, we introduce IPCC Working Group I (WGI) scenarios (for other scenarios see, e.g., Wigley, et al., 1996; O'Neill and Oppenheimer, 2002).

Five IPCC WGI scenarios (Figure 3) $\varphi(t)$ were developed to stabilize the atmospheric CO_2 at the levels of 350, 450, 550, 650 and 750 p.p.m.v. over the next few hundred years (see Schimel *et al.*, 1992 for details). Figure 4 shows the CO_2 profiles with and without corrections of the 450 p.p.m.v. IPCC scenario, produced by model (12) with data from Table 1 and $\kappa = 0.2$. Let us note that in all runs the first correction of the basic emission scenario is implemented after the peek of the atmospheric carbon concentration.

3.4 Assessment of learning rate

Let us recall that in each period m, the switch of a control in the described scenario correction stabilization procedure implies that the length of the uncertainty interval $[w_m^-, w_m^+]$ is reduced two times. Therefore the sequence of the switching times $t_1, t_2, \ldots$ – or the sequence of the inconsistency times $t_1^*, t_2^*, \ldots$ — characterizes the *learning rate* in the stabilization process; indeed, the smaller is the distance between the neighbouring times in the sequence, the faster the uncertainty is being reduced, or, equivalently, the higher is the learning rate.

For one of the IPCC WGI scenarios $\varphi(t)$, we study the learning rate, determined by the sequence of the inconsistency times $t_1^*, t_2^*, \ldots$, as a function of the parameters of the stabilization algorithm. The first inconsistency time t_1^* appears to be a monotonically increasing, practically linear, function of the target value $\hat{x}$ (see Figure 6). Therefore, we arrive at the following qualitative observation:

> *The deeper is the target value $\hat{x}$ below the initial limit value $\bar{x}$, the earlier the first inconsistency signal is received and, hence, the faster the uncertainty is reduced (twice) the first time.*

We define the *economic cost κ* for the corrections of the basic emission scenario $\varphi(t)$ as the relative value of the correction with respect to $\varphi(t)$. More accurately, we set κ to be a parameter determining the upper bound for the emission correction through $\gamma(t) = \pm\kappa\varphi(t)$, $0 < \kappa < 1$.

The *delay δ* is another important parameter of the stabilization algorithm. Figure 7 shows the second inconsistency time t_2^* as a function of the delay $\delta = t_1 - t_1^*$ between the first switching time and the time of the first receipt of the inconsistency signal. We see the following:

> *There exists an optimal value δ^* for the delay δ, at which the second inconsistency times t_2^* corresponding to different values of the cost for the correction inputs, κ, reach their minimum; moreover, at point δ^* all t_2^*'s practically coincide. In other words, the delay δ^* that is most favourable for learning after the first correction is strongly robust with respect to the cost parameter κ.*

The first switching time evidently does not depend on the cost κ; it is represented as the horizontal line in Figure 8. The length of the time interval between the second and first switching times monotonically decreases as κ grows to 1. Thus, our experiment shows the following.

> *The increase of the cost for the corrections of the basic emission scenario, κ, accelerates the learning process after the first correction.*

3.5 A modified algorithm

Figure 2 shows a strong increase of the atmospheric carbon concentration during a starting interval (in both on-line and off-line modes); eventually it goes far above the target level. At the same time, the tolerable windows approach (WBGU, 1995) implies certain bounds for the carbon concentration. Though a certain overshoot over the target value is admissible (see, e.g., Wigley, 2004), one

should try to make the peak smoother. One of the possibilities is to implement a correction from the beginning, not waiting for the first inconsistency signal.

Our numerical experiments suggest that in order to make the peak smoother, the minimal value $u = -\kappa\varphi(t)$ should be assigned till either the lower bound $\bar{w} = w^-$ is reached, or the inconsistency signal appears. Figure 5 presents the results for $\kappa = 0.2$. It is readily seen that the carbon concentration follows a much lower profile. One should not be confused by the fact that the curve goes upwards after reaching the target level: that only means that more corrections must be applied to stabilize the amount of carbon (compare with Figure 2). Like in the case of no corrections implemented in the beginning, the first switching time t_1^* is also a monotonically decreasing function of the cost κ (the grey line in Figure 8). It is however greater than the first swithing time in the case of no corrections implemented in the beginning. A summarizing conclusion is the following.

In the situation where the basic emission scenario is corrected from the beginning, the increase of the cost for corrections, κ, accelerates the learning rate in the starting period. However, at the start the learning process is slower compared to the case where the basic emission scenario in not corrected from the beginning.

4 Discussion

Finally, we list several open questions that seem to be of interest for a future study.

- Adequate continuations of the IPCC scenarios.

The IPCC WGI scenarios (see Fig. 3) were calculated (Schimel *et al.*, 1992) so as to reach certain levels of carbon concentration in the year 2300. However, the initial scenarios should be defined at a much longer time interval, which would allow one to try stabilization strategies with longer time horizons. This would make it possible to carry out a more detailed analysis of the impact of the delays, costs and other parameters of the stabilization strategies on the learning rate.

- An appropriate choice of the calibration function ν (see (9)).

As we mentioned already, a proper choice of the calibration function is crucial for specifying the learning rate.

- The sensitivity of the stabilization strategy with respect to the transition coefficients.

In this paper, we mostly studied the dependencies of the learning rate on the parameters of the stabilization algorithm under the assumption that the structure of the carbon cycle model is fixed. A next step could be a sensitivity analysis with respect to variations of the set of admissible models.

- A parametrization of the pool of admissible carbon cycle models.

This issue closely related to the previous one becomes especially important once we are interested in complementing the stabilization process with the identification of the actual model.

References

[1] Wigley, T.M.L., (2004) Modelling climate change under no-policy and policy emissions pathways, in Benefits of Climate Policies: Improving Information for Policymakers, OECD, Paris (in press)

[2] Kryazhimskiy, A., Maksimov, V., (2003) On the exact stabilization of an uncertain dynamics, Interim Report IR-03-067, IIASA, Laxenburg (available from www.iiasa.ac.at)

[3] Kryazhimskiy, A., Maksimov, V., (2004) On exact stabilization of uncertain dynamical systems, J. Inv. Ill-Posed Problems (to appear)

[4] Nordhaus, W.D., (1980) Thinking about carbon dioxide: theoretical and empirical aspects of optimal control strategies, Cowels foundation discussion paper No. 565, Yale Univ., New Haven

[5] Svirezhev, Yu., Brovkin, V., von Bloch, W., Petschel-Held, G., (1999) Optimization of reduction of global CO_2 emissions based on a simple model of the carbon cycle, Environmental Modelling and Assessment, 4. 23–33

[6] Wigley, T.M.L., Richels, R., Edmonds, J.A., (1996) Economic and Environmental Choices in the Stabilization of Atmospheric CO_2 Concentrations, Nature, 379, 240–243

[7] O'Neill, B., Oppenheimer, M., (2002) Dangerous Climate Impacts and the Kyoto Protocol, Science, 296, 1971–1972

[8] WBGU — German Advisory Council on the Global Change, (1995) Scenario for the Deviation of Global Reduction Targets and Implementation Strategies, AWI, Bremerhaven

[9] Schimel, D.C., *et al.* (1995) in Climate Change 1994: Radiating Forcing of Climate Change and an Evaluation of the IPCC IS92 Emission Scenarios (eds Houghton *et al.*), 35–71, Cambridge Univ. Press
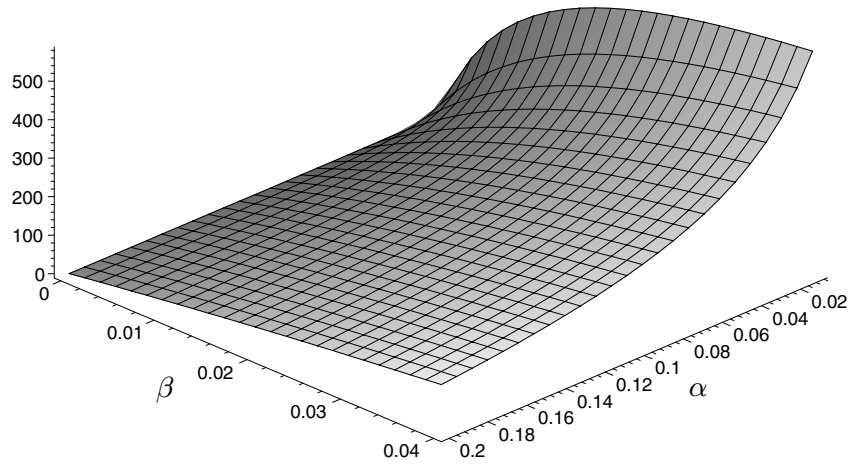
Figure 1: The landscape of the admissible limit levels for the atmospheric carbon concentration (GtC).

parameter	(a)	(b)	(c)	(IPCC450)	units
α	$1.5 \cdot 10^{-2}$	$0.95 \cdot 10^{-2}$	$0.5 \cdot 10^{-2}$	$1.5 \cdot 10^{-2}$	yr^{-1}
β	$0.25 \cdot 10^{-2}$	$0.5 \cdot 10^{-2}$	10^{-2}	$0.25 \cdot 10^{-2}$	yr^{-1}
x^0	145	145	145	145	GtC
y^0	76	500	0	76	GtC
$\hat{x}$	20	200	200	200	GtC
w^-	-1000	-800	-1000	-800	$GtC \cdot yr^{-1}$
w^+	50	50	20	50	$GtC \cdot yr^{-1}$

Table 1: The values of the model's parameters.
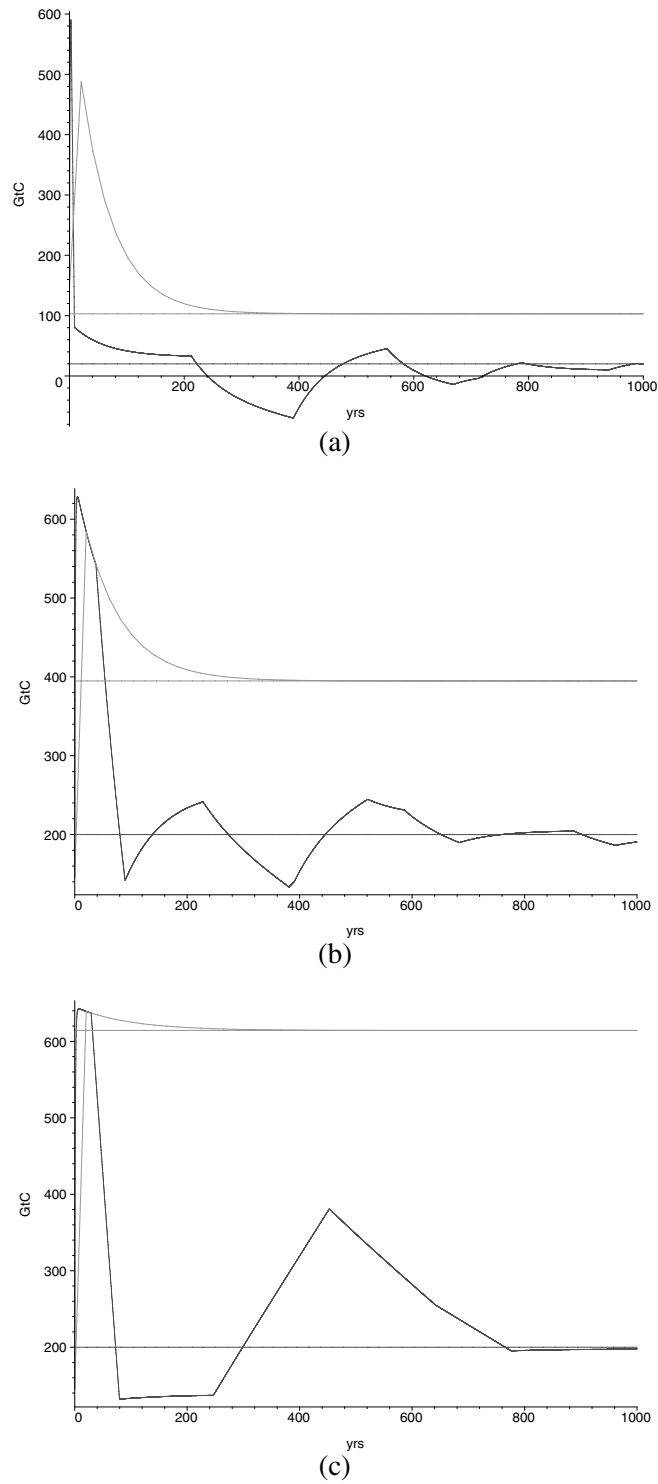
Figure 2: Three pairs of atmospheric carbon concentration trajectories, corresponding to three admissible parameters sets of the model: (a), (b) and (c) of Table 1. The trajectories driven by the off-line emission control strategy and their limit values (horizontal lines) are shown in grey. The trajectories driven by the on-line (feedback) emission control strategy and its limit values (a horizontal line) are shown in black. The limits of the off-line-controlled trajectories deviate from the target values essentially, whereas all on-line-controlled trajectories stabilize at the target levels.
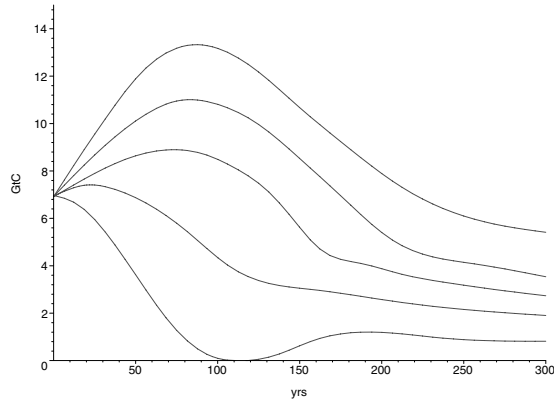
Figure 3: Five IPCC WGI scenarios corresponding to 350, 450, 550, 650 and 750 p.p.m.v. (ordered from the bottom to the top).
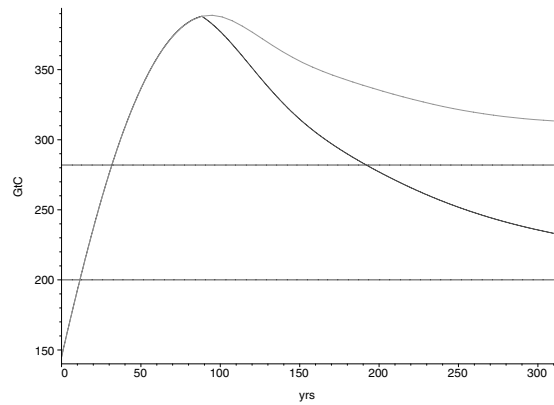

Figure 4: The grey and black curves show, respectively, the off-line- and on-line-controlled atmospheric carbon concentration trajectories corresponding to the IPCC-450 scenario parameters (Table 1); the horizontal lines show their limit values; the limit value of the on-line-controlled trajectory coincides with the target value for the atmospheric carbon concentration.
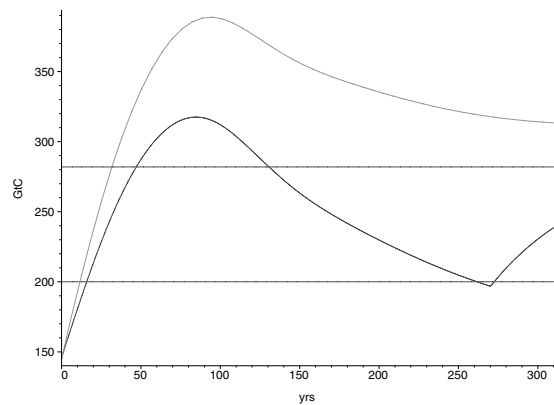

Figure 5: This figure is similar to Figure 3, with the exception that the on-line-controlled trajectory is generated by the modified stabilization algorithm.
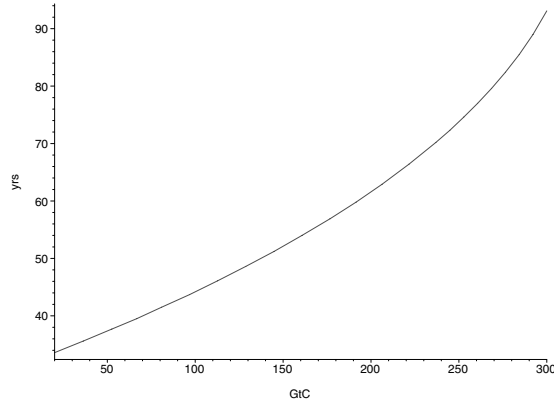
Figure 6: The first inconsistency time (at which the uncertainty in the limit of the accumulated emission is reduced two times the first time) as a function of the target value of the atmospheric carbon concentration for the IPCC-450 parameters (Table 1).
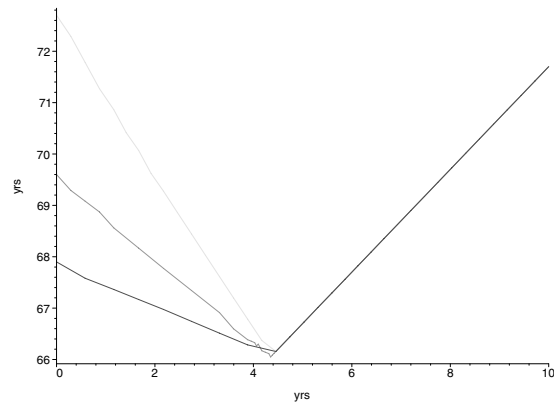

Figure 7: The second inconsistency time (at which the uncertainty is reduced two times the second time) as a function of the delay for $\kappa = 0.2$, 0.3 and 0.4 (ordered bottom-up) for the IPCC-450 parameters (Table 1).
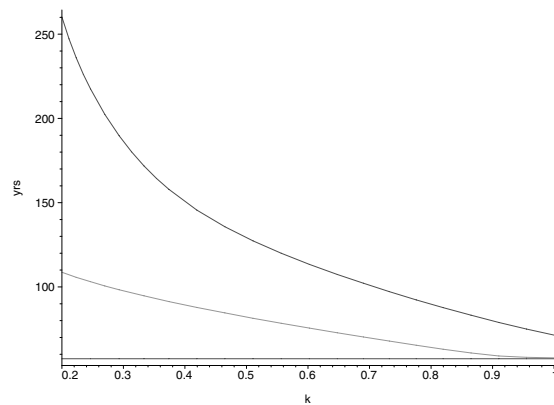

Figure 8: The black line on the bottom and the black curve on the top show, respectively, the first and second inconsistency times as functions of the target value of the atmospheric carbon concentration. The grey curve shows the second inconsistency time as a function of the target value for the modified algorithm. For simulations, the IPCC-450 parameters (Table 1) were used.

12